Physica Scripta. Vol. 35, 805–810, 1987.

Bengt Edlén's Handbuch der Physik Article – 26 Years Later†

Lorenzo J. Curtis

Department of Physics and Astronomy, University of Toledo, Toledo, Ohio 43606, U.S.A.

Received December 5, 1986; accepted January 7, 1987

Abstract

The spectroscopic methods for recognising and utilising precise regularities in atomic spectra that were presented in Bengt Edlén's classic Handbuch der Physik article "Atomic Spectra" are reviewed in the context of the present state of atomic spectroscopy. The persistence of the predicted trends is examined in the light of new data, and examples are presented which illustrate the continuing importance of these methods.

1. Introduction

It has now been 26 years since the article "Atomic Spectra" [1] was written by Professor Bengt Edlén, and this encyclopedic exposition has provided a guide to a generation of spectroscopists. The article was "intended to give a survey of empirical data in a form useful to the theorists and at the same time to provide the experimentalist with a collection of theoretical results for direct application and with efficient methods for the analysis and description of his observations". The article sought to recognise regularities among and relationships between atomic systems that could help to predict the position of unknown levels, or to interpret newly found levels. A large number of theoretical and empirical relations that could be used for this purpose were presented. In the intervening years great strides have been made in the scope and accuracy of experimental data and the sophistication of theoretical methods, which permit the validity of these approaches to be examined, and their origins and implications to be studied.

2. Semiempirical methods

Spectroscopic classification requires accurate knowledge of transition wavelengths, often to accuracies beyond parts per million. This exceeds the general capabilities of available ab initio methods, and requires the application of semiempirical methods. These techniques can be extremely accurate, and have revealed empirical regularities and linearities among members of isoelectronic and homologous sequences and Rydberg series that are not predicted by present ab initio theoretical techniques. Unfortunately these methods tend to fragment rather than to unify, since the various interactions (gross structure, electrostatic fine structure, magnetic fine structure, transition probabilities, etc.) each yield to a separate and different semiempirical modeling.

Deviations from the Coulomb potential are often phenomenologically classified as "penetration" and "polarisation", depending upon the degree of overlap between the active and passive electrons. Hydrogenlike wave functions can in many cases be utilised through a semiempirical modification that involves either a phase shift in, or a scaling of, the radial coordinate r. The phase shift corresponds to the quantum defect parametrisation, and is most effective at describing quantities that are primarily sensitive to the large r portion of the wave function (eg, gross structure, transition probabilities, high Rydberg states, etc). The radial scaling corresponds to the charge screening parametrisation, and is most effective at describing quantities that are sensitive to the small r portion of the wave function (e.g., magnetic fine structure, exchange effects, X-ray and Auger rates, etc.). Thus it is not the states themselves that are penetrating or nonpenetrating, but rather the interaction that is being studied. For a given set of term levels the gross structure and electrostatic (l-dependent) fine structure may be well described by a quantum defect formulation, whereas the magnetic (j-dependent) fine structure requires a screening parameter formulation.

An example of this is provided by gross and fine structure data for the Na isoelectronic sequence. Figure 1 presents a plot of the quantum defect relative to the yrast level ($n = 3$ for the core-occupied S and P, $n = l + 1$ otherwise) δ–δ(yrast) vs. the reciprocal square of the effective quantum number for the S, P, D and F levels, obtained from recent measurements [2] of Sr^{27+} in the Na sequence. This relative quantum defect formulation permits an exposition of the Ritz

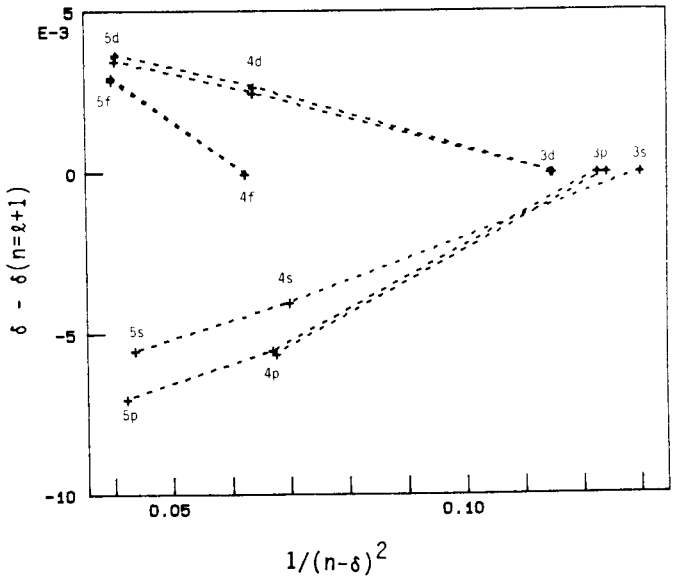

Fig. 1. Reduced quantum defect δ–δ(yrast) vs. $1/(n - \delta)^2$ for the S, P, D and F Rydberg series in Sr^{27+} (data taken from Ref. [2]). On this plot a positive slope is associated with a penetrating orbital, a negative slope is associated with a nonpenetrating (polarising) orbital.

† Presented at the "Symposium on Radiating Atoms in the Laboratory and Space" held at the University of Lund in commemoration of the 80th birthday of Professor Bengt Edlén on 2 November 1986.

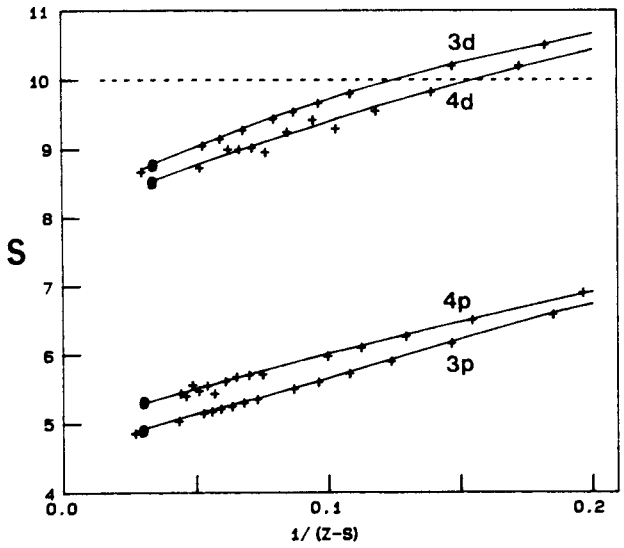

Fig. 2. Screening parameter plot of the fine structure splittings of the $3p$, $4p$, $3d$ and $4d$ terms in the Na isoelectronic sequence. A nonpenetrating term would be associated with an effective screening $S = 10$. Reduced experimental values are denoted by (+) and the Sr^{27+} values are enhanced by (O).

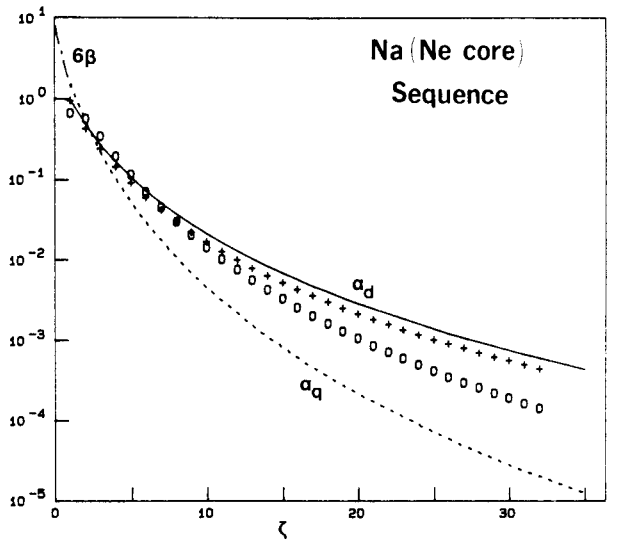

Fig. 3. Comparison of theoretical and empirical values for core polarisation parameters for the Na (Ne core) isoelectronic sequence. The theoretical curves are denoted: α_d [7] solid line; α_q [7] dashed line; 6β [5, 6] dot-dashed line. The empirical values are denoted: A [8] (+); B [8] (O).

parameter expansions of the various Rydberg series on a common plot. On this plot the sign of the derivative provides an operational definition for penetrating and nonpenetrating levels, since classical arguments imply that, for a given Rydberg series, penetration contributions should decrease and polarisation contributions should increase with increasing n (i.e., increasing orbit eccentricity). Thus it is evident from Fig. 1 that this criterion classifies the S and P levels as penetrating and the D and F levels as nonpenetrating, based upon gross structure data.

Figure 2 presents a screening parameter exposition of the fine structure data for P and D levels of a number of ions, also in the Na sequence. S is the effective screening of the nuclear charge by the core electrons, and the operational definition of a nonpenetrating term here would be $S \cong 10$, corresponding to complete screening by the 10 core electrons. This condition is satisfied by neither the P nor D terms (for low ionisation stages the D terms are actually "overscreened" with $S > 10$, due to exchange core polarisation effects). Thus for the Sr^{27+} ion, treated in Fig. 1 and designated by circles in Fig. 2, the gross energy of the D levels is classified as nonpenetrating but the fine structure is classified as penetrating.

Reference [1] provided expositions of many parametrisations of polarisation and penetration effects that yield precise predictive systematisations of spectroscopic data. A few examples will be reviewed and examined in the light of recent measurements in the sections to follow.

3. The polarisation model with penetration corrections

For states of sufficiently high l the gross energy of the active electron and the passive core are coupled only through central electrostatic interactions and the term energy T (with an appropriate spinless average over magnetic fine structure, spin multiplicity, etc.) is represented by [1]

$$T_{nl} = TH_{nl} + A\langle r^{-4}\rangle_{nl} + B\langle r^{-6}\rangle_{nl}. \qquad (1)$$

Here TH and $\langle r^{-s}\rangle$ are the term energy and radial expectation values for a corresponding hydrogenlike ion. A plot of the empirical quantity $(T - TH)/\langle r^{-4}\rangle$ vs. $\langle r^{-6}\rangle/\langle r^{-4}\rangle$ for various n with fixed l has been shown [1] to yield a straight line of slope B and intercept A, indicating that A and B are approximately constant for a given Rydberg series. For an ideally nonpenetrating case these quantities would be independent of l and could be theoretically computed (in Rydberg units for energy and Bohr units for length) as $A = \alpha_d$ and $B = \alpha_q - 6\beta$, where α_d and α_q are the dipole and quadrupole polarisabilities of the core, and β is a nonadiabatic correction for its inability to instantaneously adjust to the motion of the orbital electron. This approach has been utilised to accurately describe high l data obtained by classical spectroscopic techniques in a variety of atomic systems [1].

Generally, theoretical calculations agree well with empirical values for A, but do not agree at all with empirical values for B. This is illustrated in Figs. 3 and 4, which compare theoretical calculations for α_d, α_q and 6β with empirical values for A and B for the Na and Mg sequences. The theoretical values of α_d (Refs. [3] and [7]) are systematically slightly

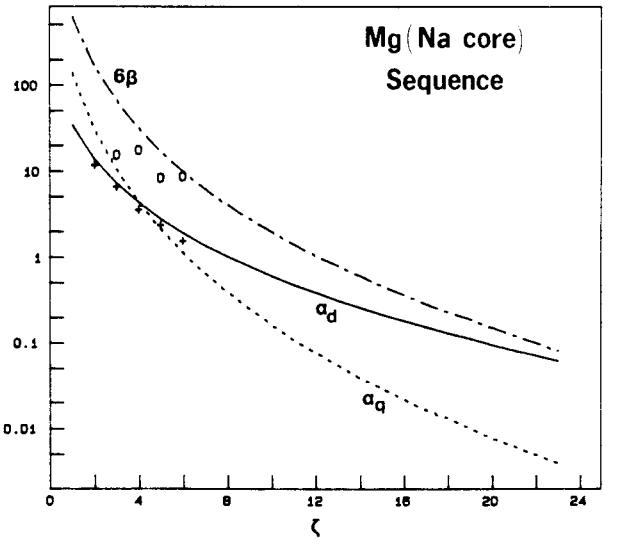

Fig. 4. Comparison of theoretical and empirical values for core polarisation parameters for the Mg (Na core) isoelectronic sequence. The theoretical curves are denoted: α_d [3] solid line; α_q [4] dashed line; 6β [4] dot-dashed line. The empirical values are denoted: A [3] (+); B [4] (O).

greater than the empirical A values (Refs. [3] and [8]) for both the Na and Mg sequences. The theoretical values of 6β (Refs. [4] and [5, 6]) exceed those of α_q (Refs. [4] and [7]) for both sequences, so $\alpha_q - 6\beta$ differs from the empirical B values (Refs. [4] and [8]) not only in magnitude, but also in sign for all ions of both sequences. Thus, either the theoretical values are inappropriate, or the measurements do not yet extend to high enough values of l, or the model is not valid.

It would be particularly valuable to apply these methods to highly ionised members of alkaline earthlike sequences. Here the large polarisabilities arising from the single out-of-shell core electron lead to well separated and easily recognisable groups of spectral lines. These lines are copiously produced in fast-ion beam spectra and would provide much-needed calibration standards if their wavelengths could be reliably predicted by the polarisation model. Unfortunately, spark spectra do not extend to the high values of l required, and there is no assurance that these results can be reliably extended without some means of accounting for penetration.

Laser and RF resonance techniques applied to neutral atoms have provided a means of testing these polarisation and penetration models. Recent $\Delta n = 0$ studies in He I [9, 10] and Ba I [11, 12] have directly probed (to within MHz accuracies) the polarisation and penetration contributions to the energy, exclusive of the gross energy. The He I case is particularly useful, since adiabatic polarisabilities and non-adiabatic corrections can be exactly calculated [13] to arbitrary order for this single electron core. These studies have provided very stringent tests of the core polarisation model and the penetration corrections, and have led to the following conclusions [10, 14]: (1) the polarisation model with theoretical polarisabilities describes the system for sufficiently high values of l, but these values are not generally accessible to classical spark sources; (2) penetration effects are approximately proportional to $\langle r^{-6}\rangle$ with a proportionality constant that depends upon l but not upon n; (3) inclusion of multipolarities higher than quadrupole worsens the agreement, suggesting a penetration-quenched truncation of the series.

These conclusions provide new insights and guidelines in the application of the polarisation model to systems more complex than the helium atom. However, these conclusions were generally anticipated by Professor Edlén, who has consistently asserted that the A and B values obtained from spark spectra should be associated with a specific Rydberg series, and warned that they should not be interpreted as theoretical polarisabilities. From conclusion (2) above it is clear that penetration effects will tend to distort empirical values of B more than those of A [15]. An extended parametrisation of penetration effects can now be made by defining the non-penetrating term value TP in the limit of a very high l as

$$TP_{nl} = TH_{nl} + \alpha_d\langle r^{-4}\rangle_{nl} + (\alpha_q - 6\beta)\langle r^{-6}\rangle_{nl} \qquad (2)$$

that uses theoretical values for α_d, α_q, and β, and contains no free parameters. To describe states of lower l, this is modified by a parametrisation of the penetration energy

$$T_{nl} = TP_{nl} + f_l\langle r^{-6}\rangle_{nl}. \qquad (3)$$

Here f_l is an empirical parameter introduced to account for penetration effects, which is a constant for each Rydberg series and decreases with increasing l. Since the intrashell $\Delta n = 0$ data that can now be directly obtained connects two Rydberg series, the standard polarisation procedure must be modified to accommodate penetration corrections pairwise. Clearly the experimental interval is the nonpenetrating interval plus the difference between the penetration corrections. For an intrashell interval between an l series and an l' series with $l' > l$, eq. (3) can usefully be written in the form

$$\Delta/\langle r^{-6}\rangle_{nl} = f_l - f_{l'}\langle r^{-6}\rangle_{nl'}/\langle r^{-6}\rangle_{nl}. \qquad (4)$$

where Δ is the effective experimental penetration energy

$$\Delta \equiv [(T_{nl} - T_{nl'}) - (TP_{nl} - TP_{nl'})]. \qquad (5)$$

A plot of these quantities for the He I data [9] is shown in Fig. 5. A joint least squares adjustment yields the values $f_D = 0.2082$, $f_F = 0.0922$, $f_G = 0.010$ and $f_H = 0$, which reproduces the measured intervals to within MHz precision.

Thus it can be concluded that the polarisation model can provide a highly precise description of high Rydberg states if used as was described in Ref. [1], including only $\langle r^{-4}\rangle$ and $\langle r^{-6}\rangle$ terms, and applying it separately to each individual l Rydberg series. The polarisation model remains a very useful approach and its modern applications extend far beyond its use in the classification of spectra. The model has been used to identify astrophysical features [16], which suggests the interesting possibility that the diffuse environment of outer space can provide a laboratory ideally suited to the determination of atomic core polarisabilities from high Rydberg states. It has been suggested that discrepancies between precise measurements and predictions of the polarisation model may permit the detection of Casimir–Polder retardation effects in high Rydberg transitions [14, 17], leading to the remarkable possibility that this simple semiclassical model could occupy a pivotal role in the testing of sophisticated relativistic and quantum electrodynamic theories.

4. Screening parametrisations

The quantum defect formulation treats the core region through its modification of the external portion of the wave function. This is not the optimum approach to the descrip-

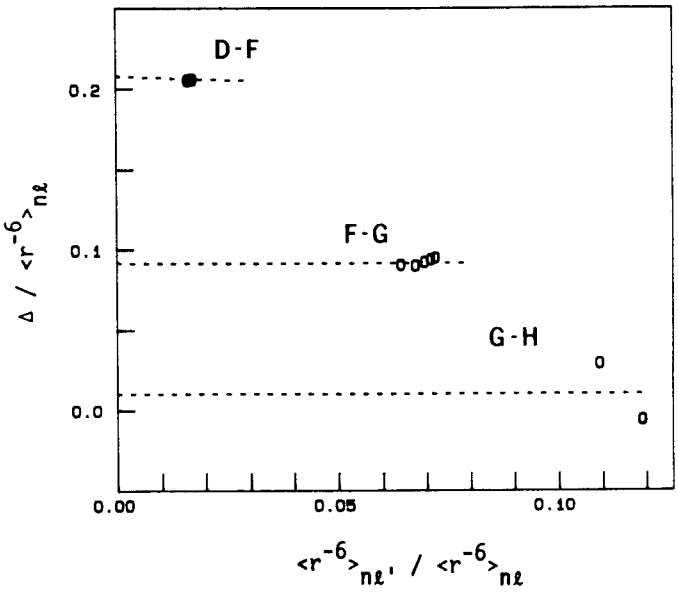

Fig. 5. Plot of $\Delta/\langle r^{-6}\rangle_{nl}$ vs. $\langle r^{-6}\rangle_{nl'}/\langle r^{-6}\rangle_{nl}$ where Δ is the intrashell difference in effective experimental penetration energies in He I. The reductions are of measured nD–nF, nF–nG and nG–nH intervals from Ref. [9]. Joint least squares fits are indicated by the dashed lines and yield penetration coefficients $f_D = 0.2082$, $f_F = 0.0922$, $f_G = 0.0010$ and $f_H = 0$.

tion of quantities that are primarily sensitive to the inner portion of the wave function. Screening parametrisations provide an alternative empirical framework better suited to the description of such quantities. In a screening parametrisation, quantum numbers retain their integer values and deviations from the independent particle model are forced to reside in an empirical effective central charge. This approach can be applied to spin-orbit energies, direct and exchange electron–electron Slater energies, and even to gross energies and transition probabilities. The magnitude and dependence of the screening parameter obtained is, however, very specific to the quantity from which it was extracted.

4.1. *Screening parameter reductions of fine structure*

The regular doublet law is the most familiar application of a screening parameterisation. It consists of mapping the fine structure separation $\Delta\sigma$ between the levels of maximum and minimum j within a term into a parameter S, defined by a screened hydrogenlike formula

$$\Delta\sigma = \mathrm{Ry}\,\alpha^2(Z - S)^4/n^3(l + 1) + \text{higher order}. \quad (6)$$

S varys much less rapidly with Z than does $\Delta\sigma$ and often exhibits regularities that would not have been suspected from the raw data. The isoelectronic regularity of S for high Z seems to improve if high order terms in the Sommerfeld–Dirac expansion [18] and QED electron self energy corrections [19] are also included. As demonstrated in Ref. [1], when the data are reduced in this manner, the empirical screening parameter is well represented by the ansatz

$$S = S_0 + S_1/(Z - S) + \ldots . \quad (7)$$

The most comprehensive base of isoelectronic fine structure data presently available is that of the Cu sequence. For this system fine structure separations have been studied through as many as 55 stages of ionisation that include the $4p$, $5p$, $6p$, $4d$ and $5d$ terms. Screening parametrisation studies have been made for each of these splittings [20]. The linearity of these S vs $1/(Z - S)$ plots persists for all Z for the nd states, but for the np states there is slight downward break in the slope at high Z. The data can be represented by two separate straight line fits, with a discontinuity in slope at $Z = 60$. MCDF calculations [21] predict the fine structure at high Z to within accuracies better than one percent, but exhibit a gentle isoelectronic curvature on this plot with neither a linear region nor a break in the slope. The empirical linearities permit predictions in the Cu sequence to within 1 part in 10^5. These results have recently [22] been combined into a common study of the following four isoelectronic fine structure intervals:

Cu sequence: $4p$ $(^2P_{1/2}–^2P_{3/2})$

Zn Sequence: $4s4p$ $(^3P_0–^3P_2)$

Ga Sequence: $4s^24p$ $(^2P_{1/2}–^2P_{3/2})$

Br Sequence: $4s^24p^5$ $(^2P_{3/2}–^2P_{1/2})$.

Since each of these intervals corresponds to a physically interpretable spin–orbit parameter ζ, they can usefully be compared both along and among these sequences. Moreover, the extensive isoelectronic data base for the Cu sequence is relevant to all four sequences, since the spin–orbit interactions that occur within its closed shell nickellike core differ from those in the Zn, Ga, and Br sequences only by the presence of $n = 4$ electrons. A study [22] has been made that combines the existing data base for these systems with *ab initio* MCDF calculations, which draws interesting conclusions.

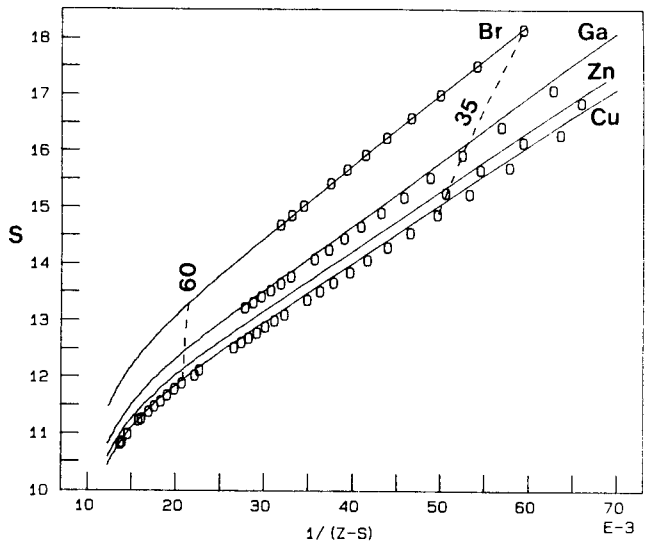

Fig. 6. Fine structure separations of the Cu, Zn, Ga and Br sequences, reduced to a screening parameter plot. The circles denote experimental measurements, the solid lines trace Dirac–Fock calculations, and the dashed lines connect the ions of Br ($Z = 35$) and Nd ($Z = 60$).

The experimental data and theoretical calculations are presented through a screening parameter exposition in Fig. 6. (This is an experimental update of the plot shown in Fig. 62 of Ref. [1], and verifies the trends predicted there.) Although data extending to and beyond $Z = 60$ exist only for the Cu sequence, the theoretical calculations for all four sequences are very similar in shape (although displaced from each other) in the region $Z > 60$. If the downturn in S beyond $Z = 60$ has its origin deep within the inner core, then the Cu sequence, which has only inner core screening, should specify this behaviour for all four sequences considered here. To test this, the screening parameter for the Cu sequence was subtracted from the corresponding quantity for each of the other three sequences to form a differential screening parameter ΔS, using both the experimental and the theoretical values. The results indicate that, although the differential plots are not linear, they are very regular. The dropoff beyond $Z = 60$ is no longer present, implying that no part of it arises from screening by $n = 4$ electrons, and suggesting that a reliable extrapolation can be made to $Z = 92$. Further, the experimental and theoretical ΔS curves are very similar in shape, and can be brought into almost exact agreement through appropriate renormalisation of the curves. This indicates a new empirical decomposition of S into separate portions arising from the core and from the active electrons, and permits measurements in one isoelectronic sequence to be used to bootstrap another sequence.

4.2. *Screening parameter reductions of exchange energies*

Screening parametrisations are not limited to the spin-orbit interaction, but can also be applied to the electron–electron direct and exchange Slater integrals. Terms of the form $nsnp\ ^{1,3}P$ in the Mg, Zn, Cd and Hg sequences are well suited to this parametrisation, since both out-of-core electrons are in the same shell and are empirically representable by the same screening constant. Tokamak and laser-produced plasma studies have recently provided useful data in these sequences. The spin–orbit energy can be parametrised as in

the alkali case. A screening parametrisation of the exchange energy can be obtained using screened hydrogenlike wave functions, yielding a linear dependence upon effective central charge with a proportionality constant that (in Rydberg units) is a calculable rational fraction. In his Handbuch article (cf. Fig. 54, pp. 170–2 of Ref. [1], Professor Edlén computed this rational fraction theoretically for $n = 2$, and evaluated its effective value from empirical data for $n = 3, 4, 5$ and 6. Modern exact machine calculations employing symbolic algebra have now been made of these rational fractions [23], and the results are very close to Edlén's empirical values, with exact-to-empirical ratios of 1.04 for $n = 3$, 0.93 for $n = 4$, 1.05 for $N = 5$ and 0.87 for $n = 6$. When specified in this manner, the screening parameters deduced from the fine structure and exchange energy are both found to be empirically linear as a function of $1/(Z - S)$ [1].

Recent measurements have permitted the semiempirical systematisations presented in Ref. [1] to be extended for the Mg [24] and Zn [25] sequences, and the persistence of the apparent linearities has thus been verified to very high stages of ionisation. Measurements for the Cd [26] sequence have recently become available, and, combined with MCDF calculations, show a similar trend [23]. These homologous sets of screening parameter reductions of isoelectronic sequence data have permitted another method of Ref. [1] to be given a modern test. Professor Edlén presented an exposition by which several sequences could be displayed on a single screening parameter plot by defining reduced axes S/N and $N/(Z - S)$ (cf. Figs. 61 and 62 of Ref. [1]), where N is a measure of the number of screening electrons. As is shown in Fig. 7, recent studies [23] indicate that a universal screening parameter plot can be made this way, that describes the Zn, Cd, and Hg sequences simultaneously. To accomplish this, it is necessary to set N equal to the total number of electrons (including both the core and the active electrons).

In the realm of very heavy and highly ionised systems, it has been predicted [27] and tentatively confirmed experimentally [28] that "hyperalkali" spectra, with a single active electron outside a closed $n = 4$ shell, are exhibited in sufficiently highly ionized members of the 61 electron Pm sequence. Similarly, "hyperalkaline earth" spectra would be expected to occur for sufficiently highly ionised members of the 62 electron Sm sequence. Although no experimental data yet exist, the same screening parametrisation of the spin–orbit and exchange energy should be applicable to this system. Accordingly these screening parameter reductions have been applied to MCDF calculations of highly ionised members of the Sm sequence, and the trends in the results were compared with homologous cases for the Mg, Zn, Cd and Hg sequences. In this manner semiempirical criteria were used to sharpen the MCDF calculations.

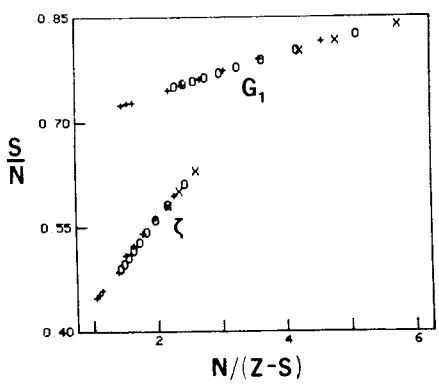

Fig. 7. Reduced exchange and spin–orbit screening parameters versus reciprocal screened charge for the Zn (+), Cd (O) and Hg (×) sequences. N is the total number of electrons (30, 48 and 80 for Zn, Cd and Hg), and its use produces a universal plot.

The trends in the screening parameter reductions of the available data can provide a means of using observations in data-rich isoelectronic sequences to judge the merit of ab initio calculations in data-poor sequences, and to combine homologous, isoelectronic and Rydberg series data together to make precise predictions.

5. Conclusions

The isoelectronic and homologous regularities indicated in Edlén's Handbuch article have been verified and their validity has been confirmed to very heavy and very highly ionised systems. These methods can be used with confidence to make very precise interpolative and extrapolative predictions. While modern ab initio MCHF and MCDF theoretical methods have become very powerful, they cannot replace semiempirical data parametrisations as evidenced by two facts: the very high accuracy requirements for spectroscopic classification cannot presently be met by theory alone; the large scale linearities manifested by the semiempirical data are usually not present in ab initio calculations. Thus the semiempirical methods presented by Professor Edlén in his Handbuch de Physik article remain the primary predictive tools of atomic spectroscopy today, and may contain clues to an improved theoretical understanding of the dynamics of complex atoms.

Acknowledgement

This work was partially supported by U.S. Department of Energy, Division of Chemical Sciences under Contract Number DE-AS05-80ER10676.

References

1. Edlén, B., in Handbuch der Physik, Vol. 27 (Edited by S. Flügge), pp. 80–220, Springer-Verlag, Berlin (1964). [This publication date is misleading, since the manuscript was delivered in final form in October 1960 (cf. footnote on p. 133 of "Topics in Modern Physics" (Edited by W. E. Brittin and H. Odabasi), Colorado Associated University Press, Boulder (1971).]
2. Reader, J., J. Opt. Soc. Am. **B3**, 870 (1986).
3. Curtis, L. J., Physica Scripta **21**, 162 (1980).
4. Curtis, L. J., Phys. Rev. **A23**, 362 (1981).
5. Bell, R. J. and Kingston, A. E., Proc. Phys. Soc. **88**, 901 (1966).
6. Eissa, H. and Öpik, U., Proc. Phys. Soc. **92**, 556 (1967).
7. Johnson, W. R., Kolb, D., and Huang, K.-N., Atom. Data Nucl. Data Tables **28**, 333 (1983).
8. Edlén, B., Physica Scripta **17**, 565 (1978).
9. Cok, D. R. and Lundeen, S. R., Phys. Rev. **A23**, 2488 (1981).
10. Curtis, L. J. and Ramanujam, P. S., Phys. Rev. **A25**, 3090 (1982).
11. Gallagher, T. F., Kachru, R., and Tran, N. H., Phys. Rev. **A26**, 2611 (1982).
12. Curtis, L. J., Ramanujam, P. S., and Theodosiou, C. E., Phys. Rev. **A28**, 1151 (1983).
13. Ludwig, G., Helv. Phys. Acta **7**, 273 (1934).
14. Curtis, L. J., Comments on Atomic and Molecular Physics **16**, 1 (1985).
15. Vogel, P., Nucl. Instr. Meth. **110**, 241 (1973).
16. Chang, E. S., J. Phys. **B17**, L11 (1984).
17. cf. Au, C. K., Feinberg, G., and Sucher, J., Phys. Rev. Lett. **53**, 1145 (1984) (and references cited therein).
18. Curtis, L. J., J. Phys. **B10**, L641 (1977).

19. Curtis, L. J., J. Phys. **B18**, L651 (1985).
20. Curtis, L. J., J. Phys. **B14**, 631 (1981).
21. Cheng, K. -T. and Kim, Y. -K., Atom. Data Nucl. Data Tables **22**, 547 (1978).
22. Curtis, L. J., Phys. Rev. A **35**, 2089 (1987).
23. Curtis, L. J., J. Opt. Soc. Am **B3**, 177 (1986).
24. Curtis, L. J. and Ramanujam, P. S., J. Opt. Soc. Am **73**, 979 (1983).
25. Curtis, L. J., J. Opt. Soc. Am. **B2**, 407 (1985).
26. Kaufman, V. and Sugar, J., Personal communication.
27. Curtis, L. J. and Ellis, D. G., Phys. Rev. Lett. **45**, 2099 (1980).
28. Träbert, E. and Heckmann, P. H., Zeits. Physik **D1**, 381 (1986).
29. Curtis, L. J., J. Opt. Soc. Am. **B3**, 1102 (1986).